

Weierstraß-Institut für Angewandte Analysis und Stochastik

im Forschungsverbund Berlin e.V.

Preprint

ISSN 0946 – 8633

Self-pinching of pulsed laser beams in a plasma filament

Carsten Brée ¹, Ayhan Demircan¹, Stefan Skupin ², Luc Bergé ³, and

Günter Steinmeyer ⁴

submitted: 1. Dec. 2008

¹ Weierstrass Institute
for Applied Analysis
and Stochastics
10117 Berlin, Germany

² Max-Planck-Institut
für Physik komplexer Systeme,
01187 Dresden, Germany

³ CEA-DAM, DIF
F-91297 Arpajon
France

⁴ Max Born Institute
for Nonlinear Optics
and Short Pulse Spectroscopy
12489 Berlin, Germany

No. 1377

Berlin 2008



2000 *Mathematics Subject Classification.* Primary 78A60, 81V80, 35Q55, 37K40 .

Key words and phrases. Nonlinear Schrödinger equations; Optical self-focusing; Ultrashort pulse propagation.

Edited by
Weierstraß-Institut für Angewandte Analysis und Stochastik (WIAS)
Mohrenstraße 39
10117 Berlin
Germany

Fax: + 49 30 2044975
E-Mail: preprint@wias-berlin.de
World Wide Web: <http://www.wias-berlin.de/>

Abstract

Competing nonlinear optical effects that act on femtosecond laser pulses propagating in a self-generated plasma filament may give rise to a pronounced radial deformation of the beam, similar to the z -pinch contraction of pulsed high-current discharges. This self-pinching locally increases the photon density. The process is further identified as the first stage in the recently observed self-compression of femtosecond laser pulses propagating in filaments. Self-pinching also explains the complicated spatio-temporal shapes generally observed in filament compression experiments.

Magneto-hydrodynamics provides effective mechanisms for increasing the electron density within high-current pulsed discharges. In the plasma channel the self-generated magnetic field may act to radially focus the electron fluence to near-thermonuclear current densities, with the z -pinch [1] being one of the most prominent examples. Such discharges have experienced an increasing degree of sophistication over the recent decades [2]. While the magnetic field is a straightforward mechanism for a dynamic increase of electron densities, no such mechanism appears at hand for increasing photon fluences. In contrast, laser pulse compression [3] has traditionally pursued energy concentration along the longitudinal axis rather than radial contraction. In the following we show that competing nonlinear optical effects inside a filament, namely Kerr-based self-focusing and plasma-induced self-defocusing, lead to a similar scenario of laser beam self-pinching. In this situation, energy is spatially contracted inside a laser pulse, giving rise to an apparent self-compression of the temporal pulse profile observed on the axis of filament propagation [4, 5].

Propagation of short pulses in a filament involves numerous linear and nonlinear optical processes that are currently modeled in the framework of an extended 2D or 3D Nonlinear Schrödinger Equation [5]. In this complex interplay it is generally difficult to isolate the primary processes leading to the observed phenomena. Utilizing the concept of characteristic lengths of the participating processes [6], however, one can sort out group-velocity dispersion, absorption, Kerr-based temporal self-phase modulation and self-steepening, leaving mainly plasma effects and transverse self-focusing and -defocusing as suspected drivers behind the experimentally observed self-compression. Such analysis, in particular neglect of dispersive effects, is indicative of vanishing energy exchange between temporal slices of a pulse in the filament. This essentially leaves particle densities and respective fluences as key parameters, similar to the situation in plasma hydrodynamics. Let us therefore restrict ourselves to analyzing radial energy flow. We use an extended Nonlinear Schrödinger Equation [7], which effectively couples the photon density to the electron density ρ . Compared to the set of full model equations [5], we neglect dissipative

terms and energy exchange between time slices, which leaves an interplay between Kerr-type self-focusing and plasma defocusing as primary dynamic effects during filament formation in gases:

$$\partial_z \mathcal{E} = \frac{i}{2k_0} \Delta \mathcal{E} + i \frac{\omega_0}{c} n_2 |\mathcal{E}|^2 \mathcal{E} - i \frac{1}{2n_0 \rho_c} \frac{\omega_0}{c} \rho(I) \mathcal{E}, \quad (1)$$

$$\rho(I) = \rho_{\text{nt}} \left(1 - \exp \left(- \int_{-\infty}^t dt' W[I(t')] \right) \right). \quad (2)$$

Here, z is the propagation variable, t the retarded time, and ω_0 is the central laser frequency at $\lambda_0 = 2\pi n_0/k_0 = 800$ nm. For the radially symmetric case, we have $\Delta = r^{-1} \partial_r r \partial_r$. n_2 is the nonlinear index of refraction. Photon densities are described via the complex optical field envelope \mathcal{E} normalized such that the intensity is $I = |\mathcal{E}|^2$. The wavelength-dependent critical plasma density is calculated from the Drude model according to $\rho_c \equiv \omega_0^2 m_e \epsilon_0 / q_e^2$, where q_e and m_e are electron charge and mass, respectively, ϵ_0 is the dielectric constant, c the speed of light, and ρ_{nt} denotes the neutral density. Plasma generation is driven by the ionization rate $W[I]$, which is suitably described by Perelomov-Popov-Terent'ev (PPT) theory [8]. For the analytical discussion and the numerical simulations, we use data for argon [5] at atmospheric pressure as parameters.

In the following, we search for a field configuration that represents a stationary state in regimes where the self-generated plasma strongly affects the filamentary dynamics. The corresponding temporal intensity profiles that maintain a balance between competing nonlinear effects in every temporal point are derived from a time-dependent variational approach, with the following trial function

$$\mathcal{E} = \sqrt{\frac{P(z, t)}{\pi R^2(z, t)}} \exp \left[-\frac{r^2}{2R^2(z, t)} + i \frac{k_0 \partial_z R(z, t) r^2}{2R(z, t)} \right]. \quad (3)$$

Here the quadratic phase guarantees preservation of continuity equations through self-similar substitutions, and the pulse radius $R(z, t)$ depends on both the longitudinal and temporal variables. For conservative systems preserving power $P(t) \equiv 2\pi \int_0^\infty I(t) r dr$ along z , straightforward algebra provides the virial-type identity [9]

$$\begin{aligned} \partial_z^2 \int_0^\infty r^3 |\mathcal{E}|^2 dr &= \frac{2}{k_0^2} \int_0^\infty r |\partial_r \mathcal{E}|^2 dr \\ &- \frac{2n_2}{n_0} \int_0^\infty r |\mathcal{E}|^4 dr - \frac{1}{n_0^2 \rho_c} \int_0^\infty |\mathcal{E}|^2 r^2 \partial_r \rho dr. \end{aligned} \quad (4)$$

Inserting the trial function (3) with $R(z, t) = w(z, t)/\sqrt{2}$ being related to the Gaussian spot size $w(z, t)$, one obtains a dynamical equation governing the evolution

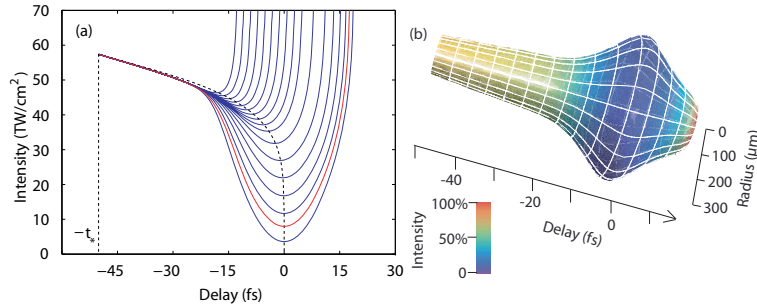


Figure 1: (a) Spectrum of solutions $I(t)$ of Eq. (5). (b) Spatiotemporal representation of the solution of Eq. (5) marked in red [see(a)], obtained by rotating the line segment generated by $R(t) = \sqrt{P(t)/\pi I(t)}$ around the t -axis. Color corresponds to on-axis intensity.

of the pulse radius R along z [9]. For the derivation of analytical expressions for the plasma term on the r.h.s. of Eq. (4), we approximate the PPT ionization rate by a power law dependence $W[I] = \sigma_{N^*} I^{N^*}$, with parameters $N^* = 6.13$ and $\sigma_{N^*} = 1.94 \times 10^{-74} \text{s}^{-1} \text{cm}^{2N^*} \text{W}^{-N^*}$ fitted to the PPT rate for the intensity range of 80 TW/cm^2 . Using $I(t) = P(t)/\pi R^2(t)$, we impose a Gaussian power profile $P(t) = P_{\text{in}} \exp(-2t^2/t_p^2)$ with duration t_p and peak input power P_{in} as a boundary condition, which results in the following integral equation for steady state solutions of the problem

$$0 = 1 - \frac{P(t)}{P_{\text{cr}}} + \mu P^2(t) \times \int_{-\infty}^t dt' \frac{I^{N^*+1}(t')}{P(t')} \frac{1}{(I(t) + N^* I(t') \frac{P(t)}{P(t')})^2}, \quad (5)$$

where $P_{\text{cr}} = \lambda_0^2/(2\pi n_0 n_2)$ and $\mu = k_0^2 N^* \sigma_{N^*} \rho_{\text{nt}}/\pi \rho_c$.

The nonlinear integral Eq. (5) is basically a generalization of a Volterra-Urysohn integral equation [10], with a kernel depending not only on $I(t')$ but also on $I(t)$. Using additional simplifying assumptions, steady-state solutions with soliton-like qualities have been previously discussed [7]. Here we solve Eq. (5) without the approximations made in Ref. [7]. Taking into account that the integral term of Eq. (5) is strictly positive, it immediately follows that nontrivial solutions only exist on the temporal interval $-t_* < t < t_*$ where $P(t) > P_{\text{cr}}$, with $t_* = (\ln \sqrt{P_{\text{in}}/P_{\text{cr}}})^{1/2} t_p$. From a physical point of view, Kerr self-focusing can compensate for diffraction only on this interval, enabling the existence of a stationary state. For computing a stationary solution $I(t)$ of the integral equation, we use the method presented in [11] which combines a Chebyshev approximation of the unknown $I(t)$ with a Clenshaw-Curtis quadrature formula [12] for the integral term of Eq. (5). As the laser beam parameters, we choose a ratio $P_{\text{in}}/P_{\text{cr}} = 2$ and a pulse duration $t_{\text{FWHM}} = \sqrt{2 \ln 2} t_p \approx 100 \text{ fs}$, leading to $t_* \approx 50 \text{ fs}$. The spectrum of solutions thus obtained is depicted in Fig. 1(a).

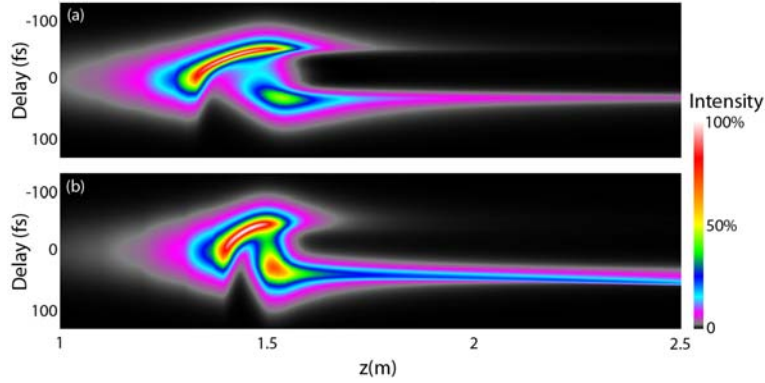


Figure 2: (a) Evolution of the on-axis temporal intensity profile along z for the reduced numerical model governed by Eq. (1). (b) Same for the simulation of the full model equations [5].

There exists a continuum of multiple roots because the problem is actually ill-posed and cannot be solved uniquely. This is due to the vanishing first term $1 - P(t)/P_{\text{cr}}$ at the boundaries. Despite the mathematical awkwardness, the spectrum of solutions exhibits some important common features. All solutions show a strongly asymmetric temporal shape, with an intense leading subpulse localized at $t = -t_*$ [7], a minimum [dashed line in Fig. 1(a)] localized near zero delay and followed by a region of rapid intensity increase, suggesting singular behavior of the solutions. The structure of the emerging solutions is exemplified in Fig. 1(b), indicating the formation of two areas of high on-axis intensity being separated by an approximately 20 fs wide defocused zone of strongly reduced intensity. Similar double-peaked on-axis intensities have frequently been observed in numerical simulations and, somewhat less pronounced, also in experiments [4, 16, 13, 15, 14].

For a deeper substantiation of our analytical model, we perform direct numerical simulations using the reduced radially symmetric evolution model Eq. (1) for the envelope of the optical field. The incident field is modeled as a Gaussian in space and time with $w_0 := w(z = 0, t) = 2.5$ mm and identical peak input power and pulse duration as used for the solutions of Eq. (5). The field is focused into the medium with an $f = 1.5$ m lens. The result of these simulations can be considered as prototypical for the pulse shaping effect inside filaments. These simulations also demonstrate that spatial effects alone already suffice for filamentary self-compression. As the evolution of the on-axis temporal intensity profile in Fig. 2(a) reveals, filamentary compression always undergoes two distinct phases. Initially, while z approaches the nonlinear focus ($z = 1.4 - 1.5$ m), a dominant leading peak is observed. When the trailing part of the pulse refocuses in the efficiently ionized zone ($\rho_{\text{max}} \approx 5 \times 10^{16} \text{cm}^{-3}$) a double-spiked structure emerges. This profile is compatible with the stationary shapes detailed in Fig. 1(a). Subsequently, only one of the emerging peaks survives and experiences further pulse shaping in the filamentary channel.

The transient double pulse structure confirms the pulse break-up predicted from the

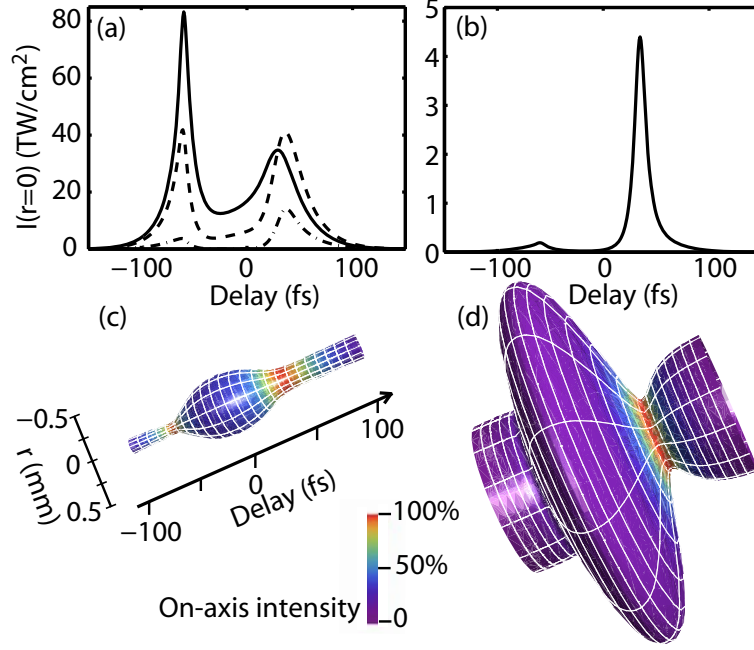


Figure 3: (a) Pulse sequence illustrating the two-stage self-compression mechanism. Shown are the on-axis intensity profiles for $z = 1.5$ m (solid line), $z = 1.55$ m (dashed line) and $z = 1.7$ m (dashed-dotted line). At $z = 2.5$ m, (b) depicts a self-compressed few-cycle pulse. (c) and (d) show the spatiotemporal characteristic of the double-spiked structure at $z = 1.55$ m and the few-cycle pulse at $z = 2.5$ m, respectively.

analysis of Eq. (5), see Figs. 3(a) and (c). At $z = 1.7$ m the leading subpulse has already been reduced to a fraction of its original on-axis intensity. This effective attenuation of the leading pulse isolates the trailing pulse that now exhibits a duration $t_{\text{FWHM}} = 27$ fs. The combined split-up and isolation during the first phase therefore already provides an about fourfold compression of the 100 fs input pulses. In the subsequent weakly ionized zone of the filament ($z > 1.6$ m), the surviving, trailing subpulse is then subject to additional temporal compression. At $z = 2.5$ m, as depicted in Fig. 3(b), our simulations indicate pulses as short as $t_{\text{FWHM}} = 13$ fs, which agrees favorably with the experimental results in Ref [4]. In contrast to the plasma-mediated self-compression in the strongly ionized zone, compression in the second zone is solely driven by the Kerr nonlinearity ($\rho < 10^{13} \text{cm}^{-3}$). With time slices of higher optical powers being able to compensate diffraction by Kerr self-focusing, these portions of the pulse diffract less rapidly than time slices with less optical power, causing the characteristically pinched spatial pulse structure in Fig. 3(d).

For an analytic description of temporal compression during the second stage of filamentary propagation, we use the dynamical equation for the time dependent beam radius derived from Eqs. (3) and (4) [9], yet neglecting the plasma term. With the initial conditions $R(z = 0, t) = R_0$ and $\partial_z R(z = 0, t) \equiv 0$ the resulting problem is analytically solvable, and we find $R(z, t) = R_0 \sqrt{1 + \xi^2(1 - P(t)/P_{\text{cr}})}$ with $\xi =$

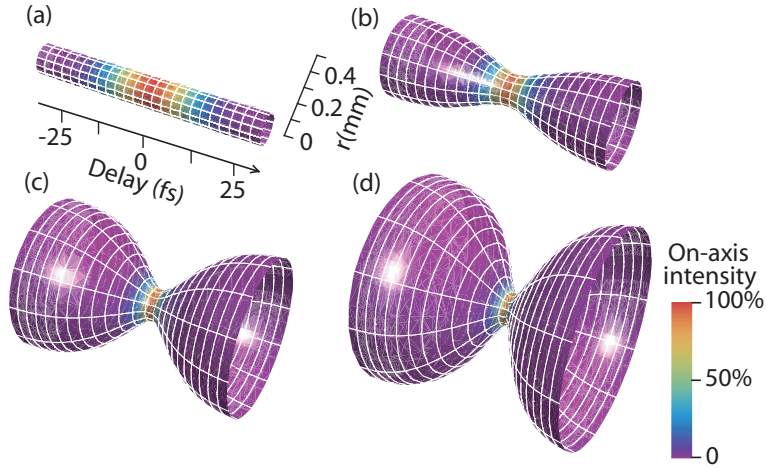


Figure 4: Sequence of pulses illustrating temporal self-compression due to Kerr-induced spatial self-pinching in the variational model corresponding to (a) $z = 1.7$ m, (b) $z = 1.9$ m, (c) $z = 2.1$ m and (d) $z = 2.3$ m.

$z/k_0 R_0^2$. This equation models the evolution of the plasma-free filamentary channel from $z > 1.6$ m. The profile $P(t)$ represents the power contained in the filament core region only. For simplicity, we assume here $P(t) = P_{cr} \exp(-2t^2/t_p^2)$, $R_0 = 100\mu\text{m}$ and $t_p = 23$ fs ($t_{\text{FWHM}} = 27$ fs). This corresponds to the duration of the pulse at $z = 1.7$ m shown in Fig. 3(a). Resulting characteristic spatio-temporal shapes are shown in Fig. 4. Self-pinching in this stage therefore serves to enhance temporal compression.

So far our analysis has completely neglected dispersion, self-steepening and losses. To convince ourselves that dissipation and temporal coupling between time slices have only a modifying effect on the discussed self-compression scenario, we pursued full simulations of the filament propagation, including few-cycle corrections and space-time focusing, cf. Ref. [5]. As shown in Fig. 2(b), minor parameter adjustment, setting $w_0 = 3.5$ mm and leaving all other laser beam parameters the same value, suffices to see pulse self-compression within the full model equations. Now self-steepening provides a much more effective compression mechanism in the trailing part. However, the comparison of Fig. 2(a) with (b) also reveals that the dynamical behavior changes only slightly upon inclusion of temporal effects. Clearly, the same two-stage compression mechanism is observed as in the reduced model. We therefore conclude that the pulse break-up dynamics in the efficiently ionized zone is already inherent to the reduced dynamical system governed by Eq. (1), contrasting previous work [13] which ascribes pulse break-up to the combined action of plasma losses and group-velocity dispersion. In fact, these effects only enhance the emergence of the discussed double-peaked pulse profiles. Moreover, rather than relying on the interplay of self-phase modulation and dispersion as in traditional laser pulse compression, filament self-compression is essentially a spatial effect, conveyed by the interplay of Kerr self-focusing and plasma self-defocusing. This dominance of spatial

effects favorably agrees with the spatial replenishment model of Moloney *et al.* [13]. However, our model indicates previously undiscussed consequences on the temporal pulse structure on axis of the filament, leading to the emergence of the pinch-like structure [Fig. 3(d)] that restricts effective self-compression to the spatial center of the filament [5, 17]. Our analysis confirms the existence of a leading subpulse, in the wake of which the short self-compressed pulse is actually shaped during the first stage of filamentary propagation. This leading structure gives rise to a pronounced temporal asymmetry of self-compressed pulses, which is confirmed in experiments [5].

Our analysis sheds new light on the rather surprising effect of self-compression, detailing the emergence of short pulses to occur in two separate steps. In a first plasma-dominated stage, the initially single-peaked pulse structure experiences refocusing in its trailing part, causing the emergence of a double-hump structure. This break-up process alone already results in an about fourfold reduction of the duration of the individual pulses. Concomitantly, a central region of the temporal pulse profile experiences strong defocusing. Choosing suitable parameters, the leading portion of the break-up is found to diffract out and reduces its intensity, while the trailing pulse can maintain a higher peak intensity. In a second Kerr-dominated stage this second pulse experiences continuing compression, which may add up to a total tenfold on-axis compression of the pulses. The main driver behind this complex scenario is a dynamic interplay between radial effects, namely diffraction, Kerr-type self-focusing, and, exclusively close to the geometric focus, plasma defocusing. The dominance of radial effects clearly indicates the unavoidability of a pronounced spatio-temporal pinch structure of self-compressed pulses. The frequently observed pedestals in this method are identified as remainders of the suppressed leading pulse from the original split-up. Our analysis also indicates that lower pulse energies < 1 mJ that require more nonlinear gases or higher pressures will see an increased influence of dispersive coupling, which may eventually render pulse self-compression difficult to achieve. Higher energies, however, do not see such limitation, opening a perspective for future improvement of few-cycle pulse self-compression schemes.

Financial support by the Deutsche Forschungsgemeinschaft, grants DE 1209/1-1 and STE 762/7-1, is gratefully acknowledged

References

- [1] V. F. D’Yachenko, V. S. Imshenik, *Rev. Plasma. Phys.* **5** (1970).
- [2] J. B. Taylor, *Phys. Rev. Lett.* **33**, 1139 (1974); W. A. Stygar *et al.* *Phys. Rev. ST Accel. Beams* **10**, 030401 (2007).
- [3] E. B. Treacy, *IEEE J. Quantum Electron.* **5**, 454 (1969); C. V. Shank, R. L. Fork, R. Yen, and R. H. Stolen, *Appl. Phys. Lett.* **40**, 761 (1982); M. Nisoli *et al.*, *Opt. Lett.* **22**, 522 (1997).

- [4] G. Stibenz, N. Zhavoronkov, and G. Steinmeyer, *Opt. Lett.* **31**, 274 (2006).
- [5] S. Skupin *et al.*, *Phys. Rev. E* **74**, 056604 (2006).
- [6] N. L. Wagner *et al.*, *Phys. Rev. Lett.* **93**, 173902 (2004).
- [7] L. Bergé and A. Couairon, *Phys. Rev. Lett.* **86**, 1003 (2001).
- [8] A. M. Perelomov, V. S. Popov, and M. V. Terent'ev, *Sov. Phys. JETP* **23**, 924 (1966).
- [9] L. Bergé and A. Couairon, *Phys. Plasmas* **7**, 210 (2000).
- [10] M. A. Darwish, *Appl. Math. Comput.* **136**, 93 (2003).
- [11] E. Babolian, F. Fattahzadeh, and E. Golpar Raboky, *Appl. Math. Comput.* **189**, 641-646 (2007).
- [12] C. W. Clenshaw and A. R. Curtis, *Numer. Math.* **2**, 197 (1960).
- [13] M. Mlejnek, E. M. Wright, and J. V. Moloney, *Opt. Lett.* **23**, 382 (1997).
- [14] S. Akturk, A. Couairon, M. Franco, and A. Mysyrowicz, *Opt. Express* **16**, 17626 (2008).
- [15] S. Akturk, C. D'Amico, M. Franco, A. Couairon, and A. Mysyrowicz, *Phys. Rev. A* **76**, 063819 (2007).
- [16] S. L. Chin, Y. Chen, O. Kosareva, V. P. Kandidov and F. Théberge, *Laser Phys.* **18**, 962 (2008).
- [17] A. Zaïr *et al.*, *Opt. Express* **15**, 5394 (2007).